The Effect of Temperature and Additive on Transport and Transformation of P of High-Phosphorus Iron Ore During Carbothermic Reduction

Yuanyuan Zhang, Qingguo Xue, Guang Wang and Jingsong Wang

Abstract Due to complicated structure and composition of high-phosphorus iron ore, pure substances were used to simulate the chemical composition of high-phosphorus iron ore to study the reaction of fluorapatite at different temperatures and effect of additives. The gasification process of P during carbothermic reduction process was investigated using a quadrupole mass spectrometer gas analysis. It is found fluorapatite was reduced to phosphorus which diffused into iron and gas phase. From the gas analysis, it was observed that PO and P gas species were vaporized around 800 °C. As the reduction temperature increased, the diffusion of phosphorus into iron was enhanced. The presence of $Ca(OH)_2$ as additives not only promoted the reduction of iron oxide, but also decreased the degree of fluorapatite reaction to inhibit P into iron.

Keywords High-phosphorus iron ore · Carbothermal reduction
Fluorapatite · Additive

Introduction

With the increasingly tension of iron ore resources, heavily dependent on imported iron ore has been restricting the development of steel industry in China. More than 7.45 billion tons high-phosphorus iron ore is mainly distributed in Hunan, Hubei,

Y. Zhang · Q. Xue · G. Wang · J. Wang (✉)
State Key Laboratory of Advanced Metallurgy, University of Science and Technology Beijing, 100083 Beijing, People's Republic of China
e-mail: wangjingsong@ustb.edu.cn

Y. Zhang
e-mail: 15841693946@163.com

Q. Xue
e-mail: xueqingguo@ustb.edu.cn

G. Wang
e-mail: 17801090926@163.com

J.-Y. Hwang et al. (eds.), *9th International Symposium on High-Temperature Metallurgical Processing*, The Minerals, Metals & Materials Series,
https://doi.org/10.1007/978-3-319-72138-5_82

Sichuan, and Yunnan Provinces of China [1, 2]. Although the grade of total iron of high-phosphorus iron ore is high, up to about 50%, but the P content reaches up to 0.3–1.8 wt%. P in the form of fluorapatite is existed with other minerals in high-phosphorus iron ore. However, due to the high temperature of the blast furnace, liquid iron absorb almost all P, thus the high-phosphorus iron ore is not suitable for the blast furnace process [3, 4].

Direct reduction process is a new method with a huge potential in the efficient utilization of high-phosphorus iron ore [5, 6]. There are some studies on the dephosphorization in direct reduction of high-phosphorus iron ore. Matinde [7, 8] used the pre-reduction and screening combined with mechanical crushing or air jet milling to process high-phosphorus iron ore. CHA [9] employed carbothermic reduction to investigate the effect of temperature, C/O molar ratio, and CaO addition on the distribution behavior of phosphorus and metallization of iron ore in the reduction process. Yu [10] treated the high-phosphorus oolitic hematite using coal-based direct reduction followed by magnetic separation, where $Ca(OH)_2$ was used as additives. Yin et al. [11]. proposed a reduction process combined with microwave and magnetic separation. However, the complex nature of high-phosphorus iron ore chemical composition and the complicated interactive relationships between gangue phases caused great difficulties for reduction mechanism of iron ore and phosphorus mineral.

Our research group is engaged in the basic research of high-phosphorus iron ore using direct reduction process. Recently it was found that C and P showed the same surface distribution in the iron phase, and the carburization and melting process of iron phase promoted each other, liquid iron had a strong ability of phosphorus absorption. It was proposed that the direct reduction temperature should be below 1148 °C to limit the P absorption of iron [12]. Based on the previous studies [13] and successful preparation of fluorapatite, the pure substances were used to simulate the chemical composition of high phosphorus iron ore in order to improve the production efficiency of high-phosphorus iron ore. During the process, direct reduction temperature was increased progressively to observe the reaction of fluorapatite and the P absorption of iron phase. Then $Ca(OH)_2$ was used to investigate the effect of additives on the reaction of fluorapatite. The gasification process of P during carbothermic reduction process was investigated using a quadrupole mass spectrometer gas analysis. In this study, the reduction process of high-phosphorus iron ore is discussed from both micro- and macro-level. A variety of analytical methods e.g., XRD, SEM-EDS were used to characterize the reduction process. This study will therefore provide the theoretical basis for dephosphorization.

Experimental

Material

The high-phosphorus iron ore used in this study was collected from western Hubei Province, China. The chemical composition and X-ray diffraction (XRD) pattern of the sample are shown in Table 1 and Fig. 1. In the first part of experiment, the

Table 1 Chemical composition of high phosphorus iron ore (wt%)

Compositions	TFe	FeO	Fe_2O_3	CaO	SiO_2	Al_2O_3	MgO	P
Content	54.08	3.42	73.46	4.26	7.77	5.07	0.74	1.15

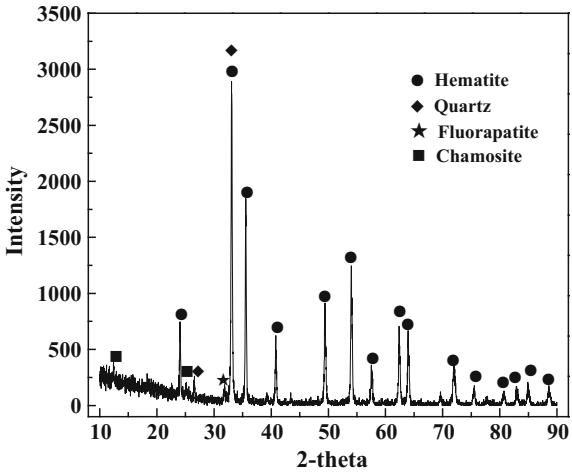

Fig. 1 XRD pattern of high phosphorus oolitic hematite

reaction of phosphorus mineral at different temperatures was investigated without additives. In the second part of experiment $Ca(OH)_2$ was added to investigate the effect of additives at a constant temperature. Pure Fe_2O_3, SiO_2, Al_2O_3, and synthetic fluorapatite [14] were used to simulate high-phosphorus iron ore. High purity graphite was used as reducing agent. The mass ratio of raw materials can be calculated through the chemical composition of high-phosphorus iron ore in Table 1. As shown in Table 2, in order to highlight the reaction of fluorapatite and other gangue minerals, the content of Fe_2O_3 was reduced and the effect of substances with a weight fraction of less than 1 wt% on the fluorapatite reaction is ignored in this study.

Experimental Procedure

Before the experiment, raw materials were mixed in accordance with simulated ratio as shown in Table 2. In the second part of experiment 5 wt% $Ca(OH)_2$ was added accordingly. 1.5 g mixture was pressed into cylindrical pellets at 16 MPa with a diameter of 8 mm and a thickness of about 10 mm. The reduction temperature was in the range of 950–1200 °C under the protection of Ar with a flow rate of 2 L/min. When the temperature stabilized, the pellets were put into an Quartz tube, then, the crucible was pushed into the furnace for 30 min.

Table 2 The material mass ratio of pure substance simulated high-phosphorus iron ore (wt%)

Raw materials	Fe_2O_3	$Ca_{10}(PO_4)_6F_2$	SiO_2	Al_2O_3	CaO	MgO	Graphite
Chemical composition of ore	73.46	6.23	7.77	5.07	0.79	0.74	–
Approximate ratio	10	1	1	1	0.1	0.1	–
Simulate ratio	5	1	1	1	0	0	1

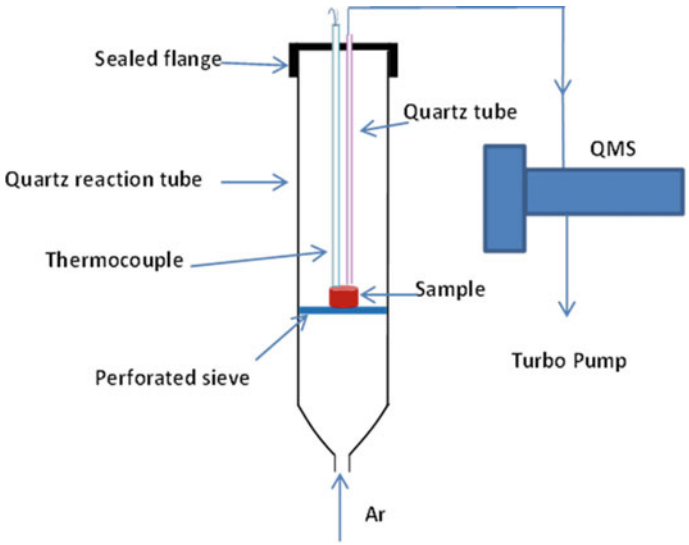

Fig. 2 Schematic diagram of the experimental apparatus

A quadrupole mass spectrometer (QMS) was used to analyze gas species vaporized during the non-isothermal carbothermic reduction of pellets without additive and pellets added 5 wt% $Ca(OH)_2$ under Ar gas conditions. Figure 2 shows the schematic representation of the experimental set up used in the gas analysis experiments. Pellets of different compositions were placed at the centre of the isothermal zone of the furnace. Then they were heated to 1200 °C under Ar atmosphere.

The phosphorus content of the pellets was measured by chemical analysis. The macroscopic analysis of pellets was investigated by X-ray diffraction (XRD). Microstructure of pellets and micro-composition analysis were observed using scanning electron microscope equipped with energy dispersive spectrometers (SEM-EDS). Dephosphorization ratio of pellets was calculated by the following formula:

$$\text{Dephosphorization ratio} = \left(1 - \frac{P_{30\text{min}} \times m_{30\text{min}}}{P_{0\text{min}} \times m_{0\text{min}}}\right) \quad (1)$$

Where P_{0min} and m_{0min} are the original P content and mass in the pellets. And P_{30min} and m_{30min} are the P content and mass in the pellets after roasting for 30 min.

Results and Discussion

Minerals Evolution of High-Phosphorus Iron Ore in Reduction Process

Macroscopic Morphology Changes and XRD Analysis of Pellets

Figure 3 shows macroscopic changes of direct reduction pellets at different temperatures. Some tiny holes were formed at the surface of pellets after reduction, caused by loss of O during reduction of iron oxide. At the reduction temperatures between 950 and 1050 °C, pellets remained compact and did not melt. When the reduction temperature reached at 1100 °C, pellets started to melt. This is because that a large amount of SiO_2 and Al_2O_3 reacted with FeO to form fayalite and spinel, which have low-melting point, as Reaction (2) and (3). The formation of low-melting point substances promoted the melting of pellets, and the mass transferring kinetic conditions of gangue phase including SiO_2, Al_2O_3, and fluorapatite were improved significantly. At the reduction temperature of 1150 °C, reduced metallic iron particles gathered and continued to grow, forming some small iron beads, and more iron beads were formed at the reduction temperature of 1200 °C.

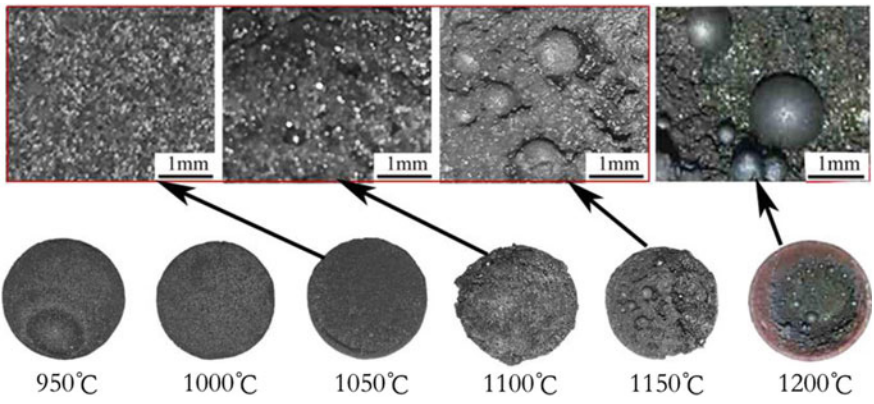

Fig. 3 Macroscopic morphology of pellets at different reduction temperatures

$$FeO(s) + Al_2O_3(s) = FeAl_2O_4(s) \quad (2)$$

$$2FeO(s) + SiO_2(s) = Fe_2SiO_4(s) \quad (3)$$

Figure 4 shows XRD patterns of pellets reduced at different temperatures. At the reduction temperature of 950 °C, diffraction peaks of fluorapatite, metallic iron, Fe_2SiO_4, $FeAl_2O_4$, and graphite were obvious, which indicates that SiO_2 and Al_2O_3 in gangue reacted with FeO to generate Fe_2SiO_4 and $FeAl_2O_4$. Compared the Gibbs free energy of Reaction (2) with Reaction (3) at 950 °C, it is clear that FeO predominantly reacted with Al_2O_3, and thus the diffraction peak of $FeAl_2O_4$ was more evident. At the reduction temperature of 1050 °C, unreacted Al_2O_3 contacted the Fe_2SiO_4 to form SiO_2 and $FeAl_2O_4$ as shown in Reaction (4), thus the diffraction peak of Fe_2SiO_4 disappeared. When the reduction temperature was increased to 1100 °C, the diffraction peak of $CaAl_2Si_2O_8$ appeared. Spinel was gradually reduced to form metallic iron and therefore some iron beads were generated. At the reduction temperature of 1200 °C, diffraction peaks of fluorapatite, $FeAl_2O_4$, and SiO_2 disappeared while the intensity of $CaAl_2Si_2O_8$ increased gradually until it was detectable in the XRD spectrum. It is likely that fluorapatite reacted with the slag. With increasing the interface tension between iron and slag, the separation of iron and slag became easier.

$$Fe_2SiO_4(s) + 2Al_2O_3(s) = 2FeAl_2O_4(s) + SiO_2(s) \quad (4)$$

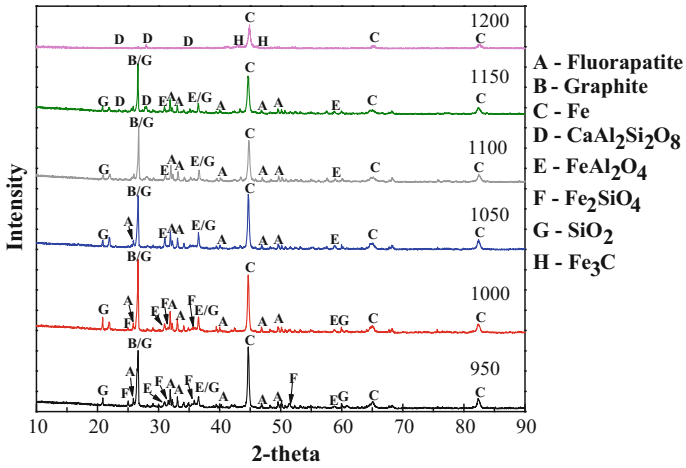

Fig. 4 XRD patterns of high-phosphorus iron ore roasted at 950–1200 °C

Microscopic Changes in Pellets and Phosphorus Content of Pellets

The reduction of pellets at different temperatures was described by XRD spectrum. However, it was difficult to make a detailed explanation about the reaction of fluorapatite. For a complete discussion, it was necessary to analyze the reaction of fluorapatite using SEM-EDS.

Microscopic changes in pellets at the reduction temperature of 950–1050 °C are shown in Fig. 5a. In this temperature range, most of P and Ca were detected in the same region, which indicates that fluorapatite was not reduced and most P was assumed to be concentrated in the form of fluorapatite in the gangue phase. As the temperature increased, iron particles grew and gathered together. The majority of metallic iron did not overlap with P. A large amount of $FeAl_2O_4$ was formed on the surface of the Al_2O_3, and needle-like fayalite appeared, the diffraction peaks of which were also detected by XRD spectrum.

Figure 5b shows the microstructure of pellets reduced at 1100 °C. The distribution behavior of P and Ca was different, which indicates that some of the fluorapatite phase was reduced to P. Thus, a lot of fluorapatite was reduced at 1100°C. However, the transfer process of P was restricted and part of P diffused into iron phase in inhomogeneous distribution. Figure 5b shows the EDS quantitative analysis of the new phase, which was determined by atomic ratio to be $CaAl_2Si_2O_8$. It was deduced that fluorapatite decomposed in the presence of SiO_2 and reacted with fayalite and spinel to form $CaAl_2Si_2O_8$ and phosphorus, according to following Reactions (5–6).

$$Ca_{10}(PO_4)_6F_2(s) \rightarrow Ca_3(PO_4)_2(s) + CaF_2(s) \tag{5}$$

$$Ca_3(PO_4)_2(s) + Fe_2SiO_4(s) + FeAl_2O_4(s) + C \rightarrow CaAl_2Si_2O_8(s) + Fe(s) + CO(g) + P(g) + PO(g) \tag{6}$$

Microscopic changes in high-phosphorus iron ore pellets at the reduction temperature of 1150–1200 °C are shown in Fig. 5c, d. As the temperature increased, more fluorapatite were reduced and a large amount of P diffused into the iron phase. P in the iron phase gradually become homogeneous. As fluorapatite reacted with other gangue minerals, the stable Ca-Si-Al gangue phase was formed, and the diffraction peak of $CaAl_2Si_2O_8$ was also detected by XRD spectrum.

The dephosphorization ratio of the roasted pellets is used to be a representative of the P changes in pellets as in Fig. 6. At the reduction temperature of 950–1050 °C, the dephosphorization ratio of the roasted pellets was about 8.56–11.97%, which is relatively low and increased moderately. At 1100 °C fluorapatite was reduced and P went into gaseous phase. As the temperature increased, more reduced P volatilized. The dephosphorization ratio of the roasted pellets increased quickly during 1100–1200 °C and reached about 25.96% at 1200 °C. That means 25.96% of the P removed from the pellets by gaseous phase.

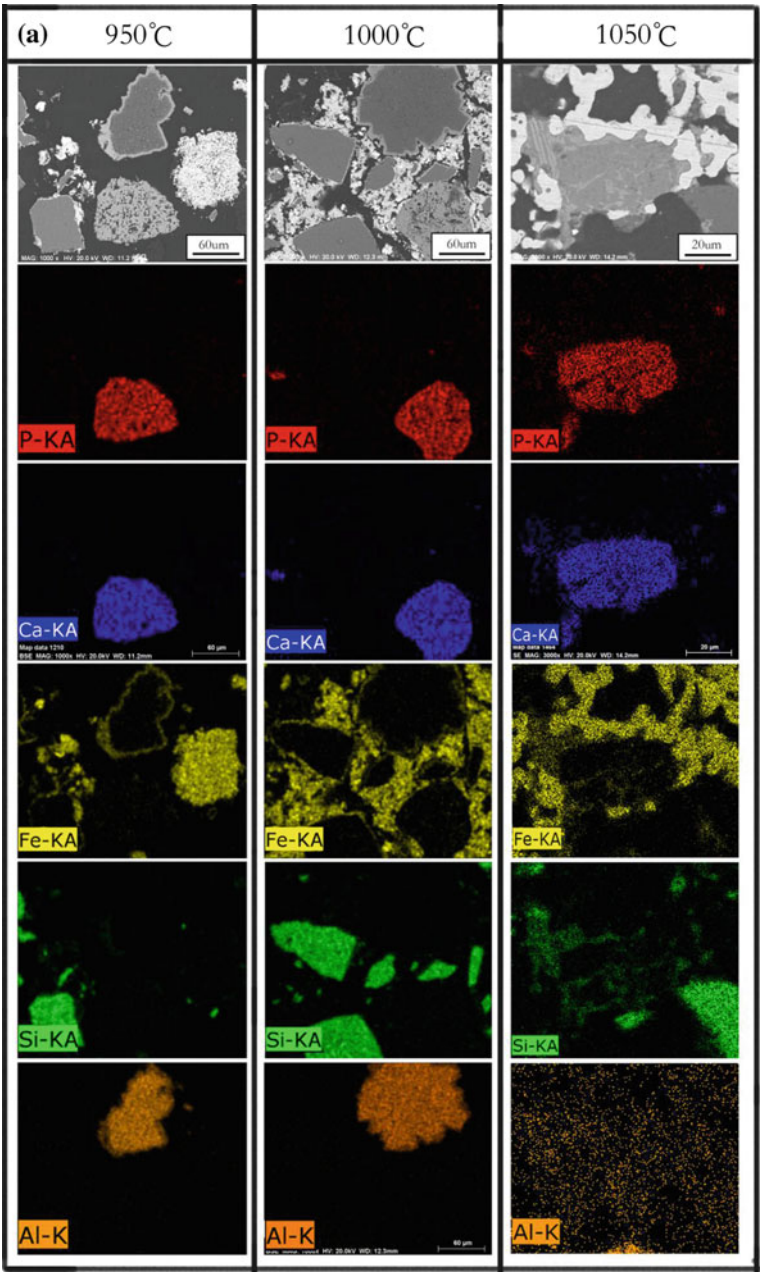

Fig. 5 Microstructure of high-phosphorus iron ore pellets reduced at 950–1200 °C

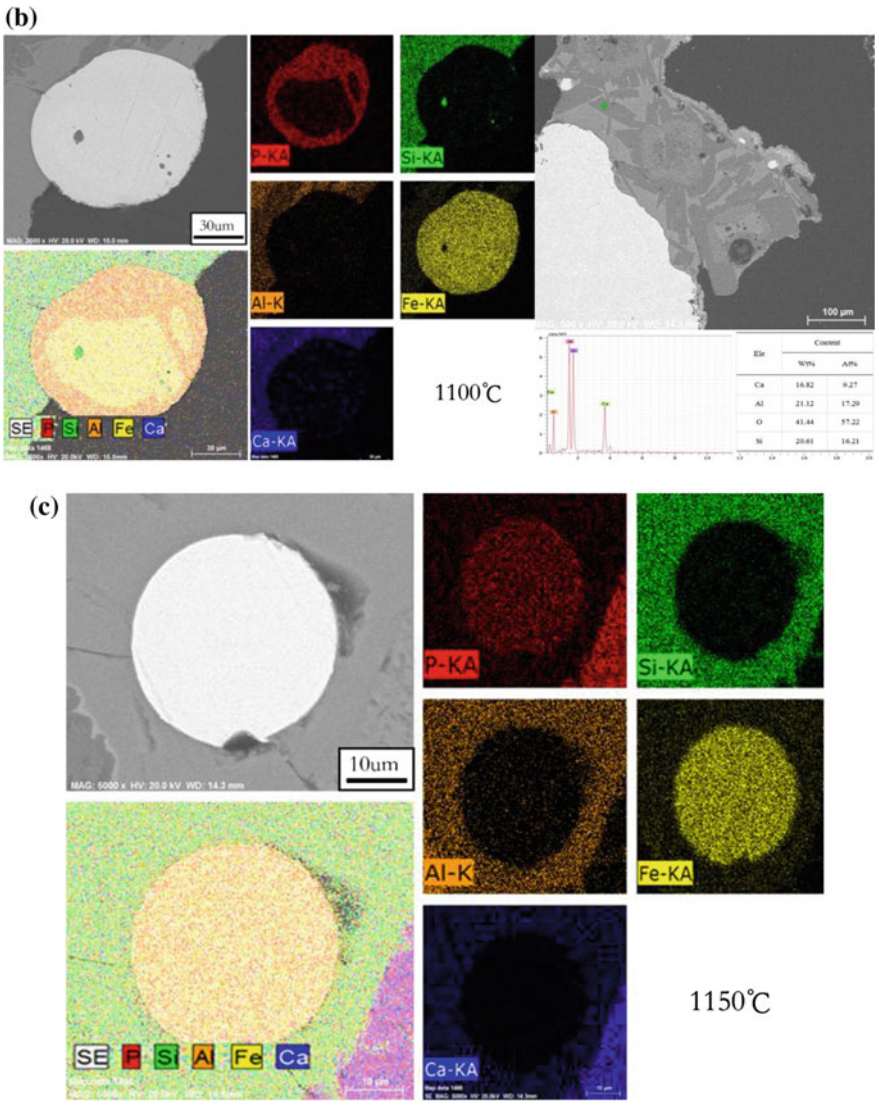

Fig. 5 (continued)

Effect of $Ca(OH)_2$ as Additives

Figure 7a shows XRD patterns of reduction pellets without additives. It can be seen from Fig. 7a that $FeAl_2O_4$ was generated by the reaction of Al_2O_3 and FeO. Hematite was reduced to metallic iron, but the diffraction peak of Fe was not evident in this case. Figure 7b shows XRD patterns of roasted pellets with 5 wt%

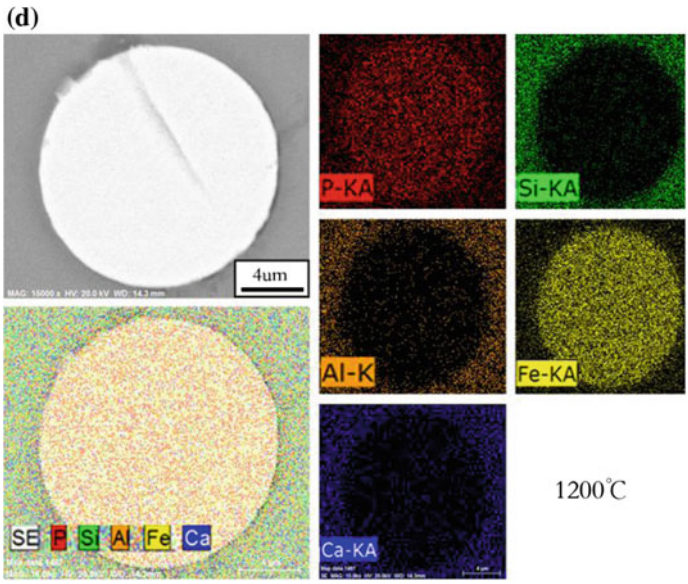

Fig. 5 (continued)

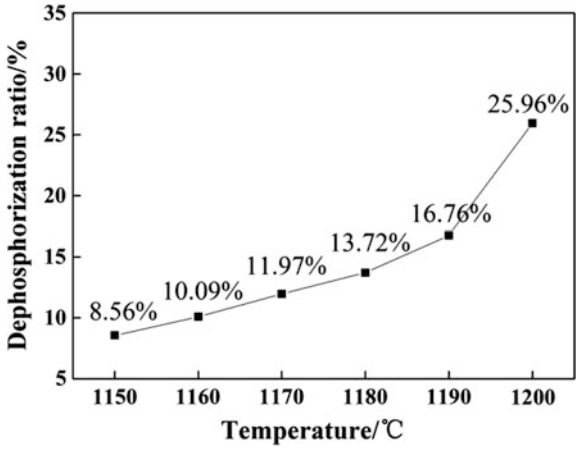

Fig. 6 Dephosphorization ratio of the carbon-bearing pellets reduced at 950–1200 °C

$Ca(OH)_2$. Diffraction peak of $FeAl_2O_4$ disappeared as CaO, dissociated from $Ca(OH)_2$, can react with $FeAl_2O_4$ to replace the FeO as shown in Reaction (7). On the other hand, diffraction peak of Fe increased markedly with 5% $Ca(OH)_2$ compared with pellets roasted without additives. Thus the reduction of iron oxide was promoted. Additionally the diffraction peak of fluorapatite increased obviously. This was attributed to the reaction between CaO and SiO_2, which promoted the reduction of fluorapatite. And the depletion of SiO_2 decreased the degree of fluorapatite reaction.

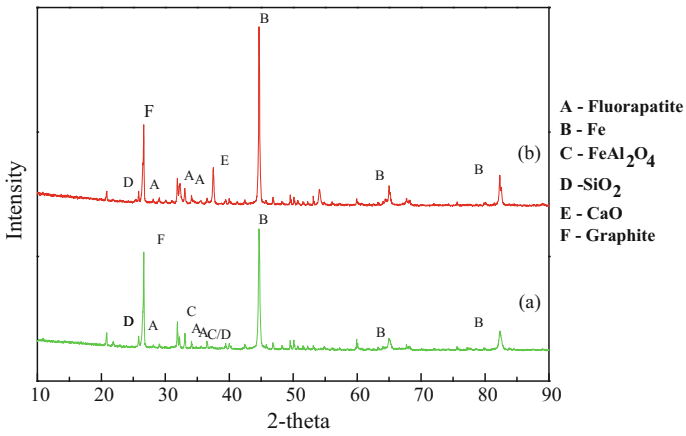

Fig. 7 XRD patterns of high-phosphorus iron ore: **a** without additives; **b** with 5 wt% $Ca(OH)_2$

$$\begin{aligned} &Fe_2SiO_4(s) + 2CaO(s) = 2FeO(s) + 2CaO \cdot SiO_2 \\ &\Delta_r G_m^{\theta} = -82,650 - 32.4T\ (J.mol^{-1}) \end{aligned} \tag{7}$$

Figure 8 shows the microstructure of high-phosphorus iron ore pellets roasted with 5 wt% $Ca(OH)_2$. It can be seen that the size of iron particles became coarser than that without additives. The area maps show that majority of Fe did not overlap with P. Al_2O_3 and SiO_2 stayed complete. P and Ca were detected in the same region, which indicated that $Ca(OH)_2$ decreased the degree of fluorapatite reaction.

Transport and Transformation of P

It can be seen from Fig. 9 that PO and P gas are generated at t about 800 °C without additive, reaching maximum respectively at 1000 and 1100 °C. This shows that in this process, the fluorapatite is reduced and the reduced P is volatilized in the form of PO and P gaseous, and part of the P enters liquid iron. However, with the addition of fluxes, the PO and P gas generation temperatures were significantly improved and did not reach the maximum. This is due to the addition of additives easy to react with silica, inhibition of fluorapatite and SiO_2 and graphite reduction reaction. Figure 10 shows the microstructure of the reduced iron, as can be seen from Fig. 10, it was found by SEM-EDS that P be in the iron produced by pellets without additive,but there is no P in the iron produced by pellets with 5 wt% Ca $(OH)_2$. Compared with Fig. 10a, b, it can be seen that the additive effectively inhibits the absorption of P by the metal iron and reduces the phosphorus content of the pearl iron.

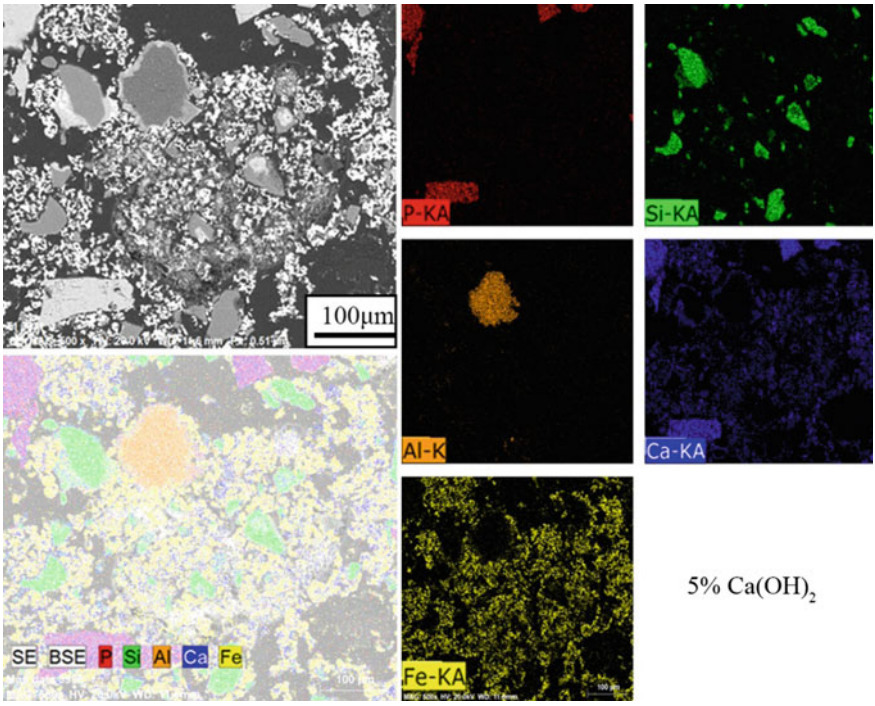

Fig. 8 Microstructure of high-phosphorus iron ore pellets roasted with 5 mass% $Ca(OH)_2$

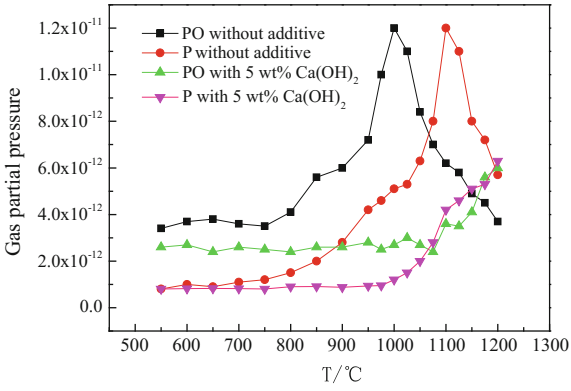

Fig. 9 Gas analysis for PO and P gas species vaporized during the carbothermic reduction reaction

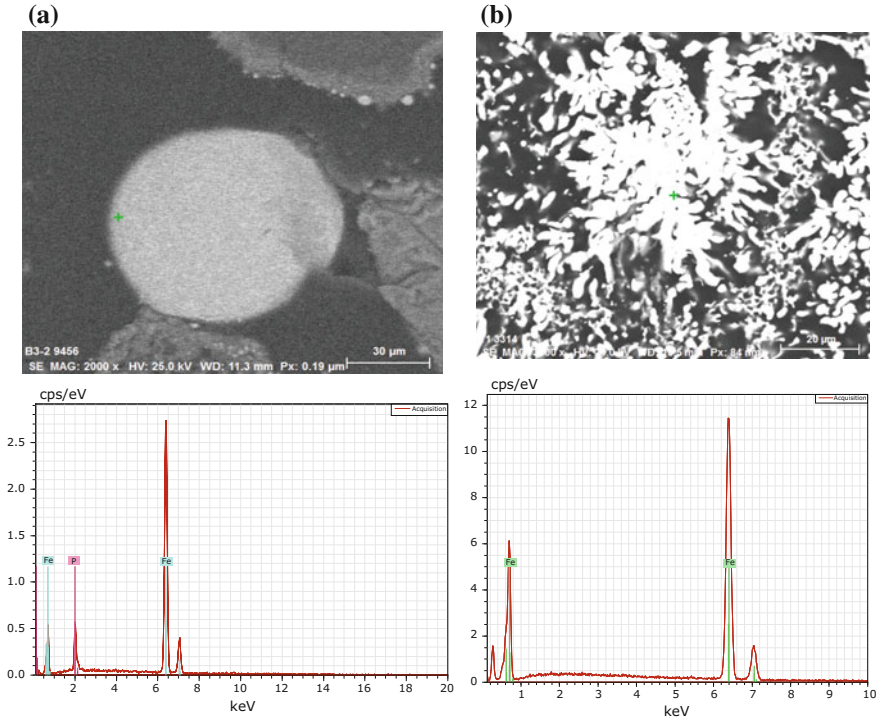

Fig. 10 Microstructure of the reduced iron: **a** without additives; **b** with 5 wt% $Ca(OH)_2$

Conclusion

Based on the experiments of effect of temperature and additive on the reaction of fluorapatite, some conclusions can be drawn as follows.

(1) At the temperature of 950–1050 °C, fluorapatite was not reduced and phosphorus was concentrated in the form of fluorapatite in the gangue phase. It was found that 1100 °C is the starting temperature for the reduction of fluorapatite contained in the high-phosphorus iron ore without additives. Fluorapatite was reduced to phosphorus which diffused into iron and gas phase at 1100 °C. As the temperature increased, the diffusion of phosphorus into iron was found to accelerate and phosphorus was reported to be distributed evenly.

(2) Iron oxide reduced firstly in the carbothermal reduction of high phosphorus iron ore, then reacted with Al_2O_3 and SiO_2 to form $FeAl_2O_4$ and Fe_2SiO_4 at low temperature. As the temperature increased, more metallic iron and the stable $CaAl_2Si_2O_8$ in slag were reported to form.

(3) $Ca(OH)_2$ contained in pellets leads to the depletion of SiO_2, which would not only promote the reduction of iron oxide, but also decrease the degree of fluorapatite reaction.

(4) PO and P gas species were vaporized around 800 °C without additive and at 1000 and 1100 °C, the amount of PO and P produced was maximized, respectively.

Acknowledgements Project was funded by the National Natural Science Foundation of China (51374024), Fundamental Research Funds for the Central Universities (FRF-TP-16-019A1) and China Postdoctoral Science Foundation(2016M600919).

References

1. Sun Y, Han Y, Gao P (2012) Exploitation situation and development trend of high phosphorus oolitic hematite. Metal Mine 3:1–5
2. Wei D (2010) Study on the ore properties of high phosphorus oolitic hematite in Western Hubei. Metal Mine 10:61–64
3. Zhang H (2013) Mineralogical properties and tendency on utilizing methods of oolitic hematite. China Metall 23(11):6–9
4. Guo HJ (2004) Metallurgical physical chemistry course. Metallurgy Industry Pres, Beijing, p 257
5. Gao W et al (2008) Present status of coal-based direct reduction and rotary hearth furnace processes. Min Metall 2:017
6. Wang G, Xue Q, Kong Lt (2013) Rotary hearth furnace iron nugget technology and its prospect in China. China Metall 23(12):6
7. Elias M, Mitsutaka H (2011) Dephosphorization treatment of high phosphorus iron ore by pre-reduction, mechanical crushing and screening methods. Int ISIJ 51(2): 220
8. Matinde E, Hino M (2011) Dephosphorization treatment of high phosphorus iron ore by pre-reduction, air jet milling and screening methods. Int ISIJ 51:544
9. Cha J-W, Kim D-Y, Jung S-M (2015) Distribution behavior of phosphorus and metallization of iron oxide in carbothermic reduction of high-phosphorus iron ore. Metall Mater Trans B 46 (5):2165–2179
10. Yu W et al (2013) The function of $Ca(OH)_2$ and Na_2CO_3 as additive on the reduction of high-phosphorus oolitic hematite-coal mixed pellets. Int ISIJ 53(3):427–433
11. Yin J et al (2012) Dephosphorization of iron ore bearing high phosphorous by carbothermic reduction assisted with microwave and magnetic separation. Int ISIJ 52(9):1579–1584
12. Cheng C et al (2015) Dynamic migration process and mechanism of phosphorus permeating into metallic iron with carburizing in coal-based direct reduction. Int ISIJ 55(12):2576–2581
13. Cheng C et al (2016) Phosphorus migration during direct reduction of coal composite high-phosphorus iron ore pellets. Metall Mater Trans B 47(1):154–163
14. Fabian R et al (1998) Preparation and chemical characterization of high purity fluorapatite. Talanta 46(6):1273–1277